

CHAPTER III

**SYNTHESIS AND CHARACTERIZATION OF GRAPHENE
OXIDE / NICKEL OXIDE NANOCOMPOSITES FOR DYE
SENSITIZED SOLAR CELL APPLICATION**

3.1 INTRODUCTION

Graphene, an atomically thin two-dimensional carbonaceous sp^2 hybridized material, has attracted tremendous attention in the research field, due to its unique electronic, electrical, and mechanical properties. These include a high specific surface area, electron transport capabilities, strong mechanical strength and excellent thermal and electrical conductivities. These unique physicochemical properties implied that it has a great potential for providing new approaches and critical improvements in the field of electrochemistry. By incorporating various metal and metal oxides like CuO, NiO, RuO₂ and Co₃O₄ nanoparticles into graphene enhance the synergistic effect between graphene / metal nanocomposites that offers great potential for various applications in the field of chemical and biological sensors, electrochemical, energy conversion and storage, solar energy harvesting [1].

Nickel oxide (NiO) nanoparticles are desirable for many applications in designing ceramic, magnetic, electro chromic and several electron transport applications. Recent studies used eco-friendly and low cost natural dyes but they still use an expensive metal as platinum as a counter electrode due to its high catalytic activity. There is a need to explore a counter electrode that is less expensive and non-corrosive in electrolyte. Hence an attempt is to use Graphene oxide/ nickel oxide as a counter electrode material [2].

3.2 MATERIALS AND METHODS

3.2.1 Materials

Graphene oxide is prepared using modified Hummers' method. Nickel oxide (NiO), Sodium hydroxide (NaOH) are purchased from Sigma Aldrich and used without further purification.

3.2.2 Synthesis of GO/NiO nanocomposites

Graphene oxide nanosheet are synthesized by a modified Hummers' method. Graphene oxide/ Nickel oxide (5:1, 5:2, 5:3, 5:4 and 5:5) nanocomposites are synthesized by dispersing 150 mg of graphene oxide in 100 ml of distilled water and are sonicated for 1 hr, followed by the addition of nickel oxide in the ratio of 5:1, 5:2, 5:3, 5:4 and 5:5 into the dispersed solution and kept under stirring for 6 hours at 60°C. This homogenous solution is kept for 12 hours at room temperature and the product is separated by centrifugation and washed with deionized water for several times, dried at 70°C for 5 hours and grinded to a fine powder [3].

3.2.3 Characterization Techniques

The crystalline structure of the prepared GO/NiO nanocomposites is studied by X-ray diffraction using X'PERT³ Panalytica diffractometer system. The FT-IR spectra are recorded for the presence of the functional groups in the nanocomposites using Shimadzu IR affinity-1. The morphology and the microstructure of the samples are studied using Field Emission scanning electron microscopy (FESEM) using a Hitachi S3000H microscope and high resolution transmission electron microscopy (HR-TEM) using Jeol JEM 2100.

3. 3 RESULTS AND DISCUSSION

3.3.1 XRD Analysis

The structural and crystalline nature of the synthesized GO/NiO (5:1, 5:2, 5:3, 5:4 and 5:5) nanocomposites are studied by X-Ray diffraction analysis (XRD). The XRD pattern of NiO and GO/NiO (5:1, 5:2, 5:3, 5:4 and 5:5) nanocomposites are shown in the Figure 3.1 (a-f). Figure 3.1 (a) represents the diffraction peaks positioned at 2θ values of 37.42° , 43.57° and 63.21° that corresponds to the (111), (200) and (220) plane respectively and are well matched with the JCPDS card no 47-1049, which confirms the formation of NiO nanoparticles. The crystallite size for NiO is found to be about 18 nm [4]. Figure 3.1 (b-f) shows the peaks at 2θ value of 11.38° , 37.42° , 43.57° , 63.21° that corresponds to the (002) plane of GO and (111), (200) and (220) plane of NiO respectively, which confirms the formation of GO/NiO nanocomposites [4].

It is observed from the XRD analysis that the intensity of the diffraction peaks corresponding to nickel oxide nanoparticles increases with the increase in the NiO concentrations for 5:1, 5:2, 5:3, 5:4 and 5:5. It is also observed that the intensity of the diffraction peak of graphene oxide 11.38° , decreases after the embellishment of nickel oxide nanoparticles on the graphene oxide surface. It is thereby confirmed that the NiO nanoparticles are well embellished on the GO nanosheet. The crystallite size of the prepared GO/NiO (5:1, 5:2, 5:3, 5:4 and 5:5) are calculated by using Debye Scherrer equation and are found to be 19 nm, 21.3 nm, 23 nm, 24 nm and 24.3 nm respectively. It is observed that crystallite size increases as the concentration of nickel oxide increases [5]. This may be due to the more number of nickel oxide nanoparticles anchored on the GO nanosheet, thereby enhancing the lattices of GO which in turn increase the crystallite size. No impurity peak is observed from XRD analysis.

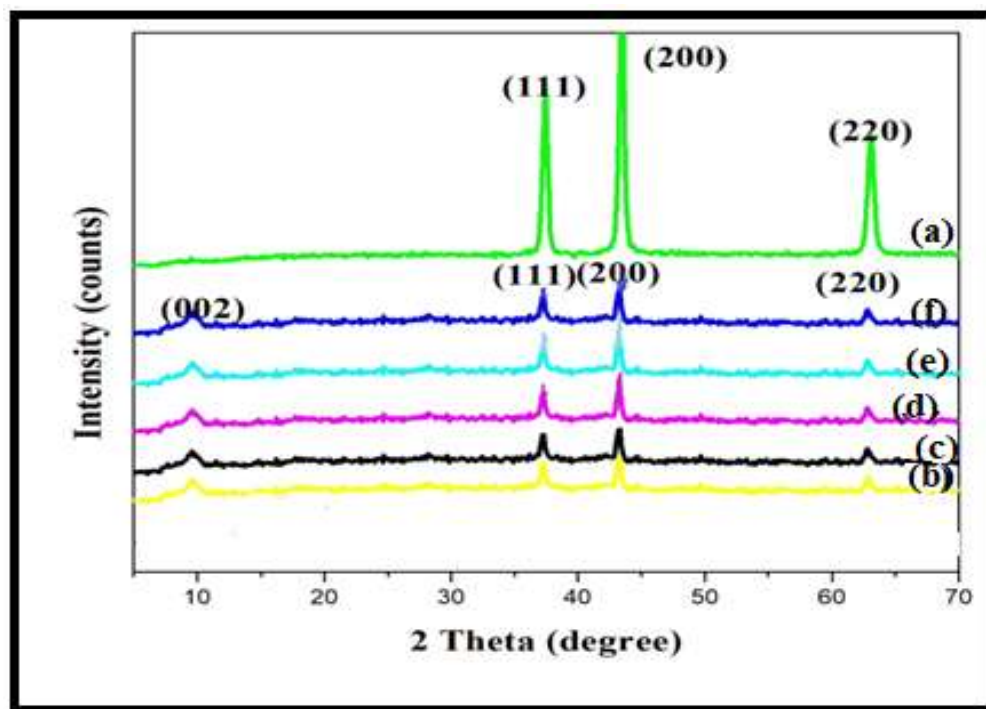


Figure 3.1 XRD spectra of (a) NiO (b) GO/NiO (5:1) (c) GO/NiO (5:2) (d) GO/NiO (5:3) (e) GO/NiO (5:4) and (f) GO/NiO (5:5) nanocomposites

3.3.2 FT-IR Spectral Analysis

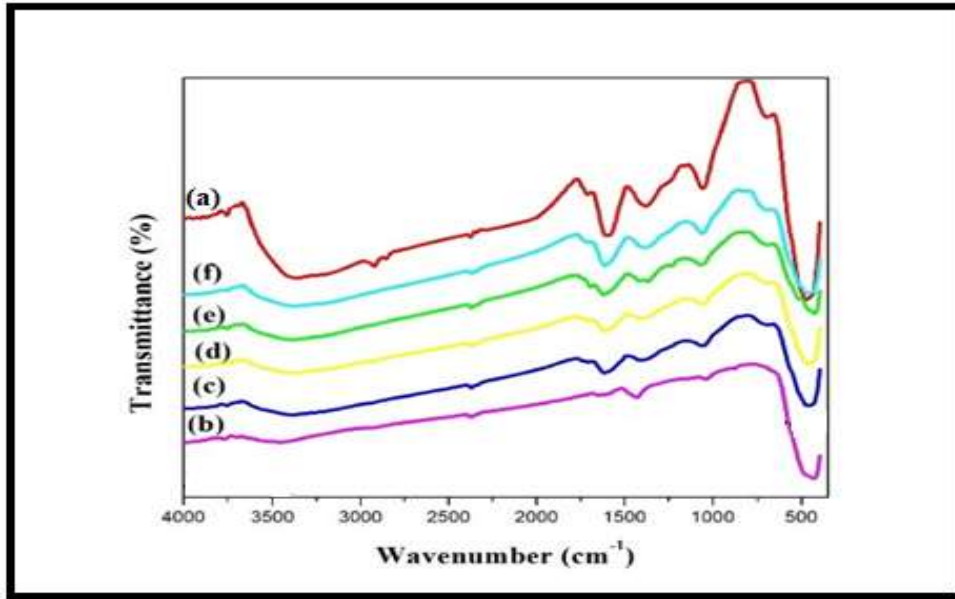


Figure 3.2(a-f) FT-IR spectra of (a) NiO (b) GO/NiO (5:1) (c) GO/NiO (5:2) (d) GO/NiO (5:3) (e) GO/NiO (5:4) and (f) GO/NiO (5:5) nanocomposites

The Fourier Transform Infrared (FT-IR) spectra of the NiO nanoparticles and GO/NiO (5:1, 5:2, 5:3, 5:4 and 5:5) nanocomposites is shown in Figure 3.2 (a-f). Figure 3.2 (a) shows the FT-IR spectrum for NiO nanoparticles and the band appeared at 480 cm⁻¹ are the metal-oxygen of Ni-O and also band observed at 1035 cm⁻¹ represents C=O vibrations which confirm the formation of nickel oxide [6]. Figure 3.2 (b-f) shows that the bands that appeared at 3654 cm⁻¹ and 1589 cm⁻¹ correspond to the stretching and bending vibration modes of O-H respectively. The band at 816 cm⁻¹ is due to Ni-O-H bending and a band at 800 cm⁻¹ is due to O=O vibration confirms the successful formation of NiO and GO/NiO (5:1, 5:2, 5:3, 5:4 and 5:5) nanocomposites. It is also observed from the Figure 3.2 (b-f) that the depth of the Ni-O band at 485 is progressively increased by increasing the concentration of NiO from 5:1 to 5:5, which confirms that the nickel oxide nanoparticles are highly spread on the GO nanosheet and that could also be evident from FESEM analysis [7].

3.3.3 Raman Spectroscopy

Figure 3.3 (a-f) shows that the Raman spectra of NiO and GO/NiO (5:1, 5:2, 5:3, 5:4 and 5:5) nanocomposites. NiO nanoparticles show broad peaks at 540 cm⁻¹

and 1070 cm^{-1} due to the Ni-O stretching mode. Figure 3.3 (b-f) shows five noticeable peaks at around 207 cm^{-1} , 357 cm^{-1} , 540 cm^{-1} , 1350 cm^{-1} and 1600 cm^{-1} which confirms the presence of GO and NiO nanocomposites. The Graphene oxide and Nickel Oxide peaks have minor shifts due to an increase in the concentration (5:1 to 5:5) of nickel oxide on the surface of Graphene oxide nanosheets [8]

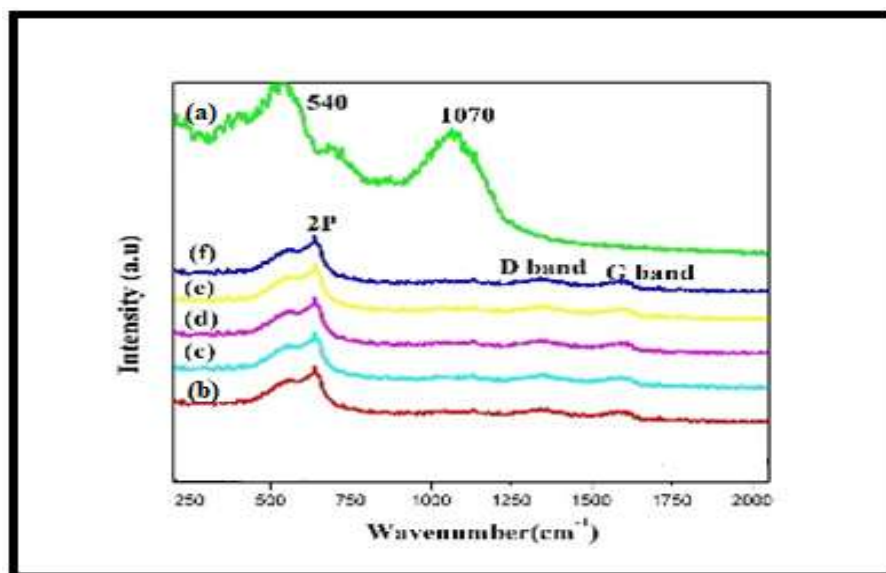


Figure 3.3 (a-e) Raman Analysis of (a)NiO (b) GO/NiO (5:1) (c) GO/NiO (5:2) (d) GO/NiO (5:3) (e) GO/NiO (5:4) and (f) GO/NiO (5:5) nanocomposites

3.3.4 FESEM

Field Emission Scanning Electron Microscopy (FESEM) analysis is performed to study the surface morphology and the shape of prepared nanocomposites. Figure 3.4 (a-f) shows the FESEM images of the prepared NiO and GO/NiO (5:1, 5:2, 5:3, 5:4 and 5:5) nanocomposites. It is observed from the Figure 3.4 (a) that the prepared NiO has flower like structure with particle size of 32 nm. Figure 3.4 (b-f) shows that the FESEM images of different concentration (5:1, 5:2, 5:3, 5:4 and 5:5) of nickel oxide nanoparticles decorated on the Graphene oxide nanosheet [9]. It is also observed that the number of NiO nanoparticles on the surface of GO nanosheet is found to be increased with increase in the concentration from 5:1 to 5:5. FESEM analysis also confirmed that the 5:5 concentrations of NiO nanoparticles are highly blended on the large surface area of Graphene oxide nanosheet without impurities helps to increase the efficiency of GO/NiO nanocomposites in DSSCs.

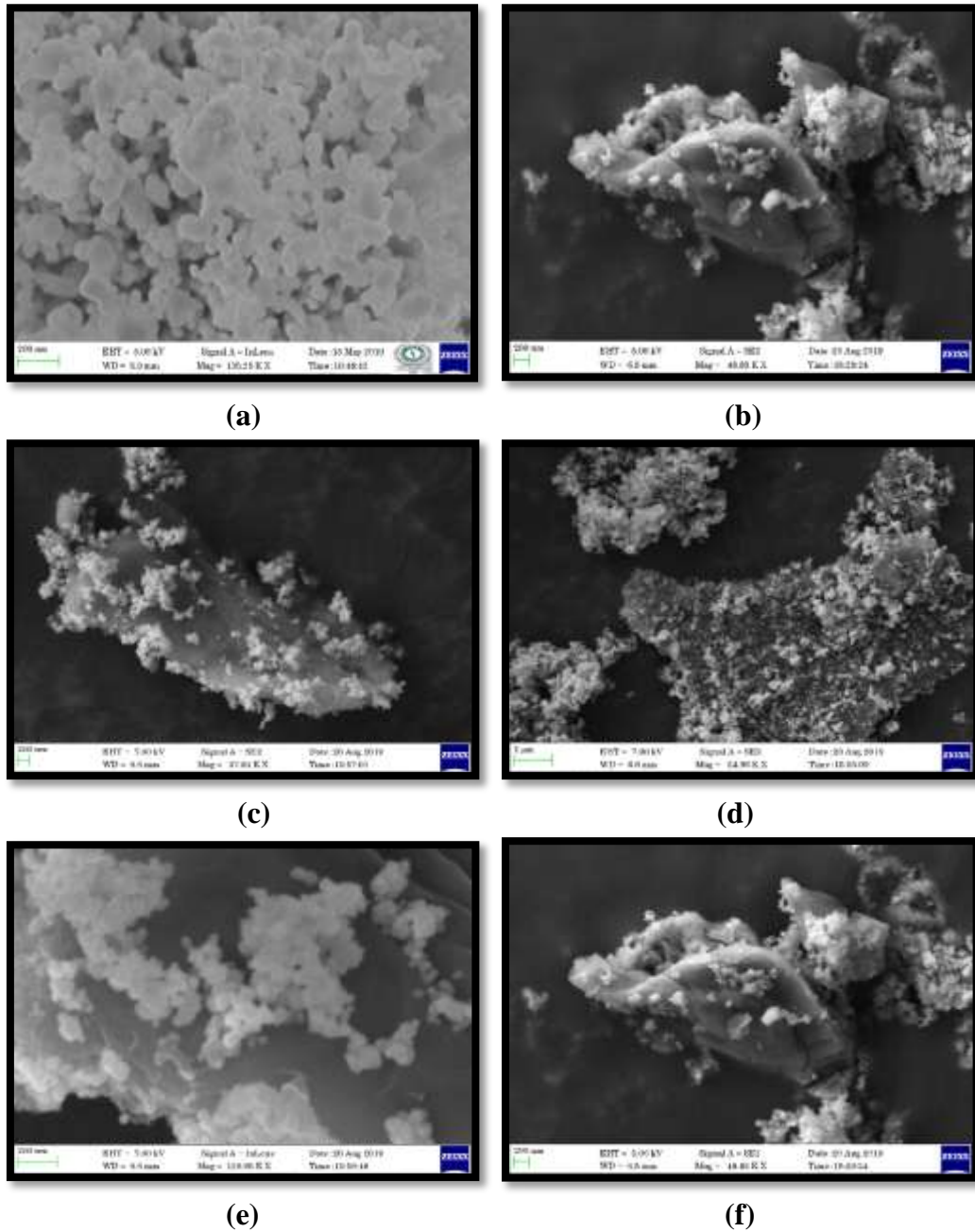
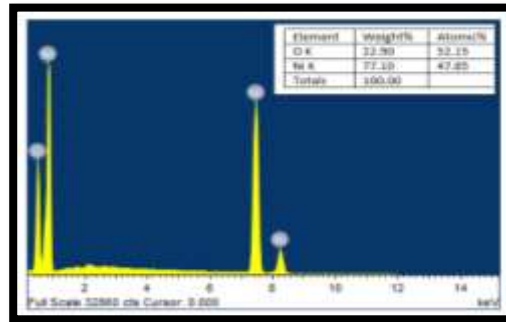


Figure 3.4 FESEM images of (a) NiO and (b) GO/NiO (5:1) (c) GO/NiO(5:2) (d) GO/NiO (5:3) (e) GO/NiO (5:4) and (f) GO/NiO (5:5) nanocomposites

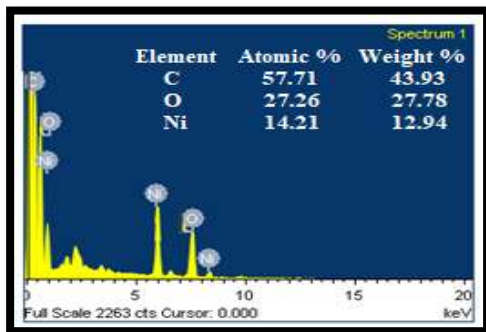
3.3.5 EDX Analysis

The EDX analysis is used to identify the elemental presence in the prepared nanocomposites. Figure 3.5 (a-f) represents the EDX spectra of NiO and GO/NiO (5:1, 5:2, 5:3, 5:4 and 5:5) nanocomposites. Figure 3.5 (a) confirms the presence of Ni and O elements without any impurities as also evidenced from XRD analysis. Figure 3.5 (b-f) shows the presence of C, O, and Ni that confirms the formation of

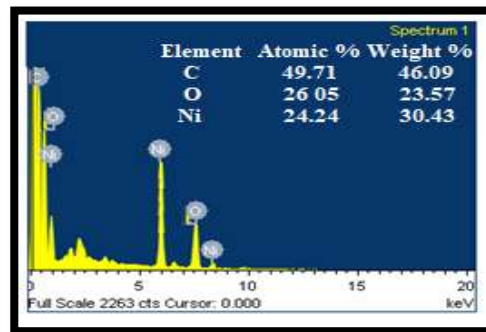
GO/NiO (5:1, 5:2 5:3, 5:4 and 5:5) with the atomic and weight percentage are given as inset table. It is observed that the number of nickel and oxygen atoms increases with increase in the concentration of nickel oxide nanoparticles on the surface of GO.



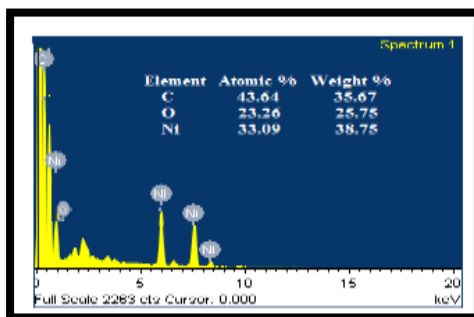
(a)



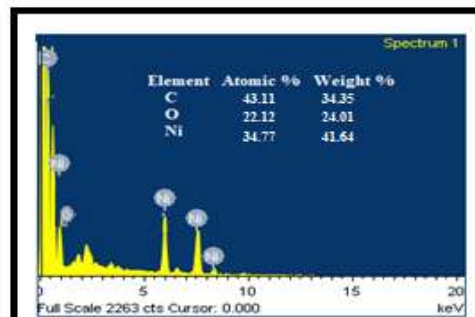
(b)



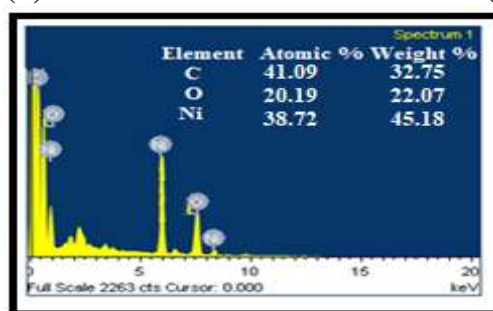
(c)



(d)



(e)



(f)

Figure 3.5EDX spectra (a) NiO (b) GO/NiO (5:1) (c) GO/NiO (5:2) (d) GO/NiO (5:3) (e) GO/NiO (5:4) and (f) GO/NiO (5:5) nanocomposites

3.3.6 HR-TEM Analysis

Figure 3.6 (a-c) shows that the HR-TEM images of the GO/NiO (5:4) nanocomposites. It confirms that the Nickel oxide nanoparticles are well distributed on the surface of GO nanosheet and are also evidenced from the FE-SEM analysis. It is further observed from the Figure 3.6 (a-c) that the rod structure of NiO nanoparticles are equally spread on the surface of GO nanosheet. The distributed nickel oxide nanoparticles are homogeneous without any agglomeration. This confirms the successful formation of GO/NiO (5:5) nanocomposites [10,11].

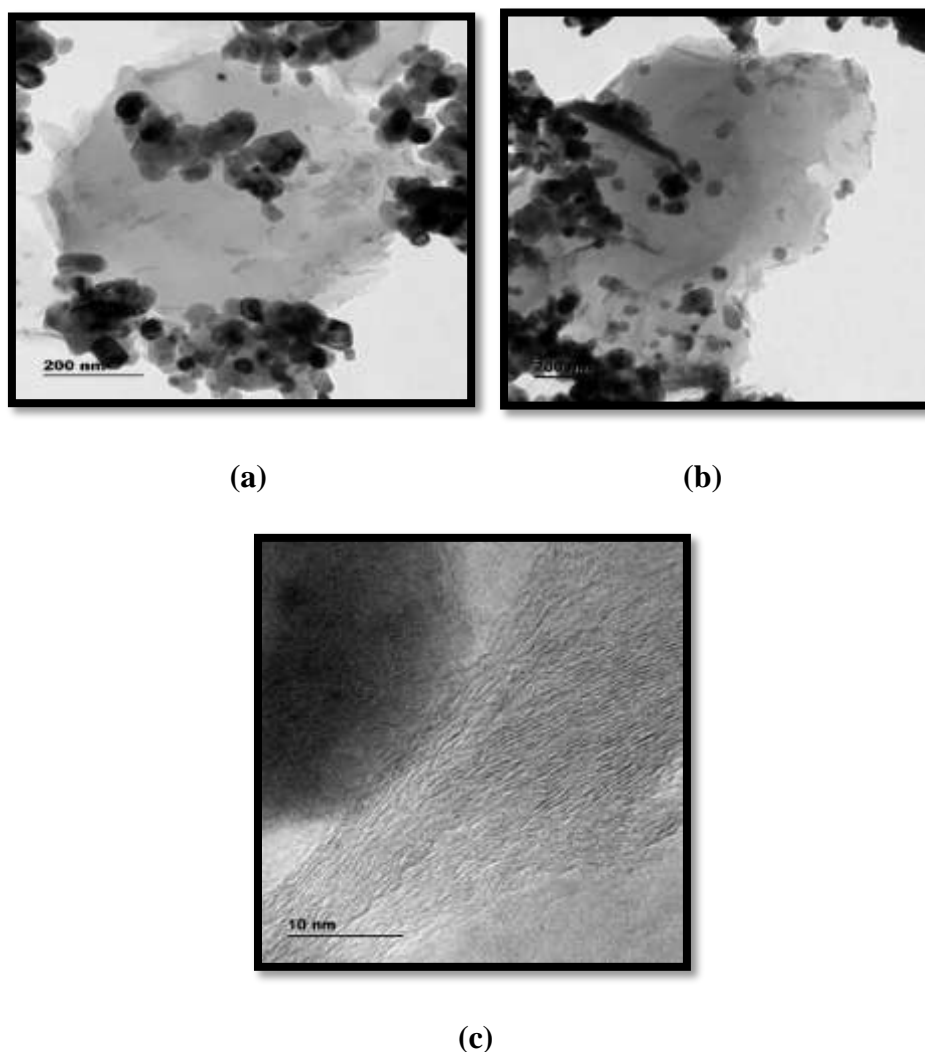


Figure 3.6 (a-c) HRTEM images of (a-c) GO/NiO (5:4) nanocomposites

3.3.7. Selected Area Electron Diffraction Analysis

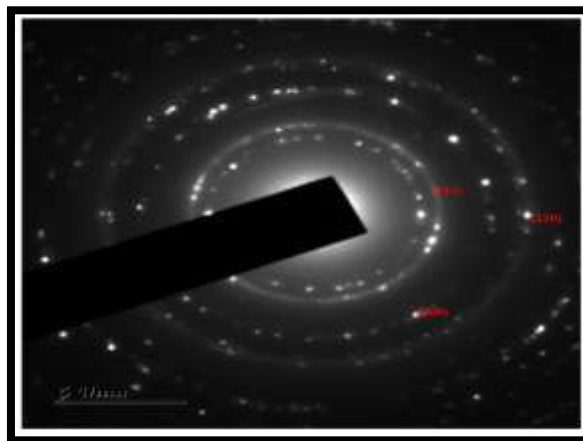


Figure 3.7 (a) SAED image of Graphene oxide/ Nickel oxide nanocomposites

The selected area electron diffraction pattern (SAED) of the prepared nanocomposites GO/NiO (5:5) is shown in the Figure 3.7 (a). It is observed from the Figure 3.7 that there are three discrete bright rings which indicate the successful formation of a well crystalline face centered flower like the structure of Nickel oxide nanoparticles on the surface of graphene oxide nanosheet. Each ring corresponds to the (111), (200) and (220) planes of nickel oxide nanoparticles, which could also be evidenced from XRD analysis [12].

3.4 CONCLUSION

This chapter describes the Graphene oxide / Nickel oxide (5:1, 5:2, 5:3, 5:4 and 5:5) nanocomposites prepared by chemical precipitation method. The XRD analysis shows that the prepared nanocomposites are crystalline in nature and the average crystallite size of NiO and GO/NiO (5:1, 5:2, 5:3, 5:4 and 5:5) nanocomposites is found to be 18 nm, 19 nm, 21.3 nm, 23 nm 24 nm and 24.3 nm respectively. FE-SEM and HR-TEM analysis revealed that the NiO nanoparticles are successfully embellished on the Graphene oxide nanosheet. The elemental analysis confirmed the different concentrations of Nickel oxide nanoparticles and Graphene oxide elements in the prepared nanocomposites without any impurities. This work confirms the simple preparation of GO/NiO (5:1, 5:2, 5:3, 5:4 and 5:5) nanocomposites and this prepared nanocomposite can be used as a counter electrode for Dye Sensitized Solar Cell Applications.

REFERENCES

1. R. Kawano and M. Watanabe, *Chem. Commun.* , 330 (2003).
2. L. Wang, H. Zhang, R. Ge, C. Wang, W. Guo, Y. Shi, Y. Gao, and T. Ma, *RSC Advances* 3, 12975 (2013).
3. D. Xu, H. Zhang, X. Chen, and F. Yan, *J. Mater. Chem. A* 1, 11933 (2013). [44]
D. Shi, N. Pootrakulchote, R. Li, J. Guo, Y. Wang, S. M. Zakeeruddin, M. Grätzel, and P. Wang, *The Journal of Physical Chemistry C* 112, 17046 (2008), <https://doi.org/10.1021/jp808018h> .
4. F. Sauvage, S. Chhor, A. Marchioro, J.-E. Moser, and M. Graetzel, *Journal of the American Chemical Society* 133, 13103 (2011), PMID: 21702510, <https://doi.org/10.1021/ja203480w>.
5. F. Fabregat-Santiago, J. Bisquert, E. Palomares, L. Otero, D. Kuang, S. M. Zakeeruddin, and M. Grätzel, *The Journal of Physical Chemistry C* 111, 6550 (2007), <https://doi.org/10.1021/jp066178a>
6. X. Chen, D. Xu, L. Qiu, S. Li, W. Zhang, and F. Yan, *J. Mater. Chem. A* 1, 8759 (2013)
7. F. Bella, S. Galliano, C. Gerbaldi, and G. Viscardi, *Energies* 9, 384 (2016).
8. M. Willgert, A. Boujemaoui, E. Malmstrom, E. C. Constable, and C. E. Housecroft, *RSC Advances* 6, 56571 (2016).
9. Y. Rong, X. Li, G. Liu, H. Wang, Z. Ku, M. Xu, L. Liu, M. Hu, Y. Yang, M. Zhang, T. Liu, and H. Han, *Journal of Power Sources* 235, 243 (2013).
10. O. Bagheri, H. Dehghani, and M. Afrooz, *RSC Advances* 5, 86191 (2015).
11. S. Chaurasia, C.-T. Li, M. B. Desta, J.-S. Ni, and J. T. Lin, *Chemistry-An Asian Journal* 12, 996 (2017), <https://onlinelibrary.wiley.com/doi/pdf/10.1002/asia.201700039> .
12. R. A. Senthil, J. Theerthagiri, J. Madhavan, and A. K. Arof, *Ionics* 22, 425 (2016).